Adv. Space Res. Vol. 6, No. 3, pp. 157–175, 1986
Printed in Great Britain.

0273–1177/86 $0.00 + .50

PLASMA TRANSPORT IN THE PLASMASPHERE

J. Lemaire

IASB, 3 avenue Circulaire, B–1180 Bruxelles, Belgium

ABSTRACT

The plasmasphere is filled with very low energy plasma upwelling from the topside ionosphere. The field-aligned distribution of this thermal ionospheric plasma is controlled by the gravitational and centrifugal potential distribution. There are two extreme types of hydrostatic plasma distribution in this field-aligned potential : the Diffusive Equilibrium distribution and the Exospheric Equilibrium distribution corresponding respectively to a saturated and to an almost empty magnetic flux tube. As a result of pitch angle scattering by Coulomb collisions an increasing number of ions escaping from the ionosphere are stored on trapped orbits with mirror points at high altitudes in the low density region. As a result of collisions the field-aligned density distribution gradually changes from exospheric equilibrium with a highly anisotropic pitch angle (cigar like) distribution to a diffusive equilibrium with a nearly isotropic pitch angle distribution. It is shown that the suprathermal ions become anisotropic much more slowly than ions of energies smaller than 1 eV. The Coulomb collision times have been estimated for flux tubes at different L values. A numerical simulation of the flux tube refilling process has been presented. The diurnal variation of the equatorial plasma density has been illustrated for plasma elements convected along drift paths which have a large dawn- dusk asymetry. The formation of a Light Ion Trough is discussed. Finally, evidence has also been given for the existence of a 'plasmaspheric wind' corresponding to a slow subsonic and continuous radial expansion of the plasma stored in the plasmasphere.

INTRODUCTION

The plasmasphere is filled with cold plasma. This plasma is mainly of ionospheric origin. This means that it has been produced in the ionosphere by photoionization and eventually escapes from the topside ionosphere into the protonosphere and magnetosphere along dipole magnetic field lines. In addition to this field-aligned motion of plasma all these thermal particles experience an azimuthal drift perpendicular to the magnetic field direction.

ON MAGNETIC FIELD LINES "FROZEN-IN"...

For the low energy ions and electrons (< 10 eV) the electric drift velocity is much larger than the gradient-B and curvature drift velocities ($\underline{V}_B$ and $\underline{V}_C$). Therefore, for a given electric and magnetic field distribution, all charged particles spiraling along a given magnetic field line drift with almost the same velocity $\underline{V}_E = \underline{E} \times \underline{B}/B^2$. At any later instant of time, these same particles will be found on another field line which is the same for all these particles (see Fig.1). Another more popular way to put this is to say that the magnetic field line 'moves' with the plasma convection speed $\underline{V}_E$, and that all particles are confined to this moving magnetic field line.

Of course, this implies that the particles have almost 'zero energy'! Indeed, particles with non-zero energies experience additional gradient-B and curvature drifts which are energy dependent (see Fig.1). For instance, an electron with an energy E_2 drifts eastwards with a larger drift velocity than the electron with the energy E_1 ($< E_2$). Therefore, both particles will not remain on the same 'moving' magnetic field line. The particles of different energies and of different charges will therefore be dispersed over a range of different field lines whose separation will increase with time, as illustrated in Fig.1. This strictly means that a collisionless plasma can be considered as 'frozen in the magnetic field' only when its particles have strictly zero energy, otherwise the usefulness of the MHD 'frozen-in concept' is of course questionable if not misleading, as already voiced by Alfvèn /1/. But since plasmas of zero temperature or with zero velocity dispersion are not very common in nature, the usefulness of this concept is necessarily very limited, indeed.

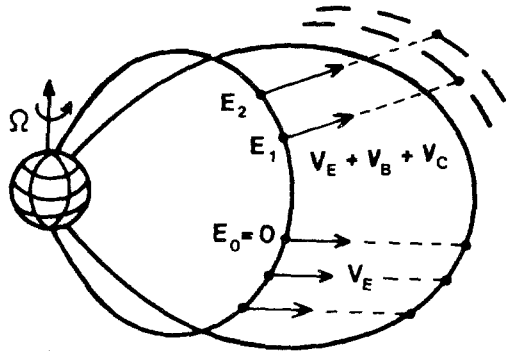

Fig.1 : Charged particles of zero energy ($E_o = 0$) are "frozen in" magnetic flux tubes "moving" with the electric convection velocity $\underline{V}_E = \underline{E} \times \underline{B}/B^2$; but particles of non-zero energies $E_1 > E_2 > E_0$ in a plasma element do not stay in the same "moving" magnetic flux tube.

ION-EXOSPHERES IN HYDROSTATIC EQUILIBRIUM

Let us nevertheless consider almost zero energy particles and ignore dispersion resulting from gradient-B and curvature drifts ; after all, this seems to be a good first approximation for plasmaspheric particles whose energy does not exceed 10 or 100 eV !

Let us then catch one of these magnetic field lines 'moving' with the $\underline{E} \times \underline{B}/B^2$ drift velocity and travel around the world with this immaterial string. If the L value of the magnetic flux tube within which we are 'frozen-in' is not too large (e.g. $L < 4$) our co-moving frame of reference is then corotating almost with the angular speed of the Earth. The plasma looks stationary all around of us, unless there is field aligned plasma flow. This flow of plasma must come from the ionosphere. This is expected to happen when the plasma density in the flux tube is rather low and in the process of refilling with fresh ionospheric plasma. But we may also observe plasma moving toward the ionosphere when too much plasma has been accumulated in the magnetosphere or when magnetic flux tubes are squeezed as a result of earthward convection toward a region where the magnetic field intensity is higher.

On very rare occasion we may see plasma which is almost stationary, i.e. in hydrostatic equilibrium. In this case, the field-aligned velocity of the plasma is equal to zero. This is probably exceptional because of the ever present north-south asymmetries of the

geomagnetic field lines as well as dissimilar boundary conditions in the conjugate ionospheres at the feet of magnetic flux tubes ; nevertheless let us first consider the distribution in a flux tube under the condition of hydrostatic equilibrium, i.e. when there is no mass flow in any direction along the magnetic field direction.

If hydrostatic equilibrium is satisfied the plasma density decreases exponentially with altitude from a rather high value of the order of 10^6 cm^{-3} at the altitude of the F-region (300 km) to a value of the order of 300 cm^{-3} in the equatorial plane at L = 4. The density gradient is characterized by a scale height which is proportional to $T_e + T_i$, the sum of the electron and ion temperatures, and inversely proportional to the gravitational force : $H = k(T_i + T_e)/mg$. Note that it is the projection of the gravitational force along the local magnetic field direction which determines the actual field-aligned density scale height. This field- aligned component of the gravitational force depends therefore on the dip angle which is a function of latitude along the field line.

Field-Aligned Potential

Since we are in a corotating frame of reference which is accelerated, the pseudo centrifugal force that each particle experiences in addition to the gravitational force has also a projection along the direction of $\underline{B}$ as pointed out in an early study by Angerami and Carpenter /3/. The field- aligned component of the sum of the gravitational and centrifugal forces can be derived from a generalized potential ϕ_g which is given by

$$\phi_g(r,\lambda) = - \frac{GM_E}{r} - \frac{1}{2} \Omega^2 r^2 \cos^2\lambda + c^{te} \qquad (1)$$

where Ω is the local angular velocity of the plasma, G is the gravitational constant, M_E is the mass of the Earth, r is the radial distance and λ is the dipole latitude. Taking into account the ambipolar diffusion electric field in a hydrostatic and corotating ion-exosphere, it can be shown that the difference of potential energy for a proton or electron between two points of latitude λ_o and λ located along the field line L is given in eV by

$$\psi = - \frac{0.324}{L} \left[\frac{1}{\cos^2\lambda} - \frac{1}{\cos^2\lambda_o} + \frac{1}{3} \left(\frac{\Omega}{\Omega_E}\right)^2 \left(\frac{L}{L_c}\right)^3 (\cos^6\lambda - \cos^6\lambda_o) \right] \qquad (2)$$

where Ω_E is the angular speed of the Earth, and $L_c = (2GM_E/3\Omega^2 R_E^3)^{1/3}$.

Figure 2 gives the value of ψ as a function of latitude along 5 different field lines. Along the innermost magnetic field lines (L = 2, 3, or < 5.78) the total potential energy is an increasing function of altitude (solid lines in figure 2). Along these field lines the ion density and electron density is a decreasing function of altitude with a minimum in the equatorial plane.

Zero-Parallel-Force Surface

However, for the field lines at L > 5.78 in a corotating ion exosphere, ψ has a minimum in the equatorial plane and two conjugate maximum at non-zero latitudes. The points where ψ is maximum are those where the magnetic field line crosses the Zero Parallel Force (ZPF) surface whose cross section is shown in figure 3. These points correspond to the places where the parallel component of $\underline{g}$ is balanced by the parallel component of the centrifugal force.

Lemaire /8/ called this surface the Roche limit surface. Indeed, by analogy with the astrophysical Roche limit this is the locus of points where a droplet of fluid would split into two pieces under the action of the centrifugal and gravitational force of a

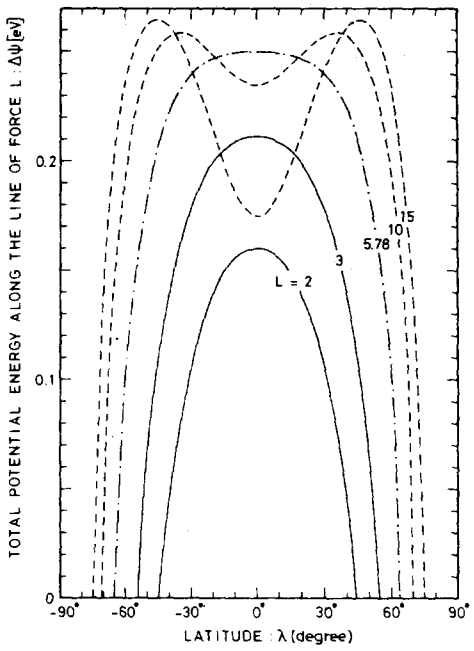

Fig.2 : Gravitational plus rotation potential energy of H^+ ions along different magnetic field lines corotating with the Earth. For $L \leq 5.78$, the total potential ψ, has maximum value in the equatorial plane at $\lambda = 0$; for $L > 5.78$, ψ has a minimum at the equator and two symmetrical maxima out of the equatorial plane at $\lambda = \lambda_m$ /8/.

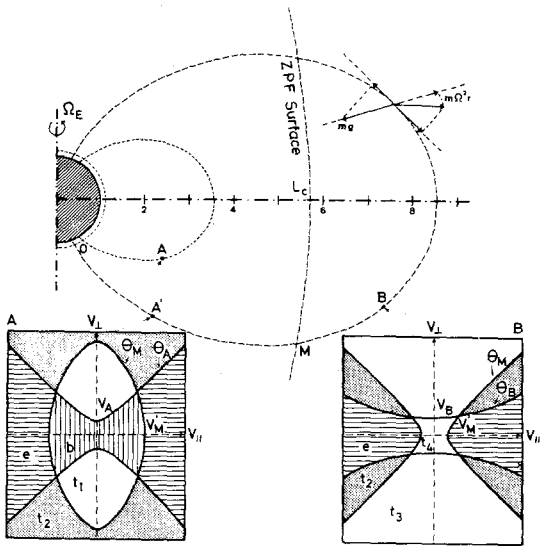

Fig.3 : Two dipole magnetic field lines : L = 3.5 and L = 8.5. The meridional cross-sections of the Zero-Parallel-Force (ZPF) surface where the field aligned component of the gravitational and centrifugal force are equal. L_c is the equatorial distance of the ZPF surface. $L_c = 5.78$ for an ion-exosphere corotating with the Earth's angular velocity (Ω_E). The two panels show the different regions in the velocity space corresponding to the different classes of charged particles, below the ZPF surface (at A, and A') and above the ZPF surface (at B). V_A and V_B are the minimum perpendicular velocities of trapped particles, respectively at A and B ; V_M is the minimum parallel velocity of an escaping particle at A or B. θ_A and θ_B are the minimum pitch angles of trapped particles, respectively at A and B ; θ_M is the maximum pitch angle of an escaping particle at A or B /9/.

binary system. But in our case the mass of one of these binary objects is made equal to zero; furthermore, there is another difference between the traditional Roche Limit and that introduced in the case of rotating ion-exosphere in a dipole magnetic : i.e., the r^{-3} variation of the cross-section of magnetic flux tubes, as compared to the r^{-2} cross-section of gravitational flux tubes. To avoid confusion Lemaire /10/ has suggested this surface be renamed the Zero Parallel Force surface (ZPF).

Beyond this ZPF surface the field-aligned component of the total force is directed outwards, while inside this surface, closer to the Earth, the gravitational force dominates the centrifugal force.

Different Classes of Orbits

Very low energy (< 2 eV) charged particles spiraling along magnetic field lines are very sensitive to these gravitational and centrifugal forces. Their trajectories in this total potential field depend very much on their kinetic energy ($\frac{1}{2}$ mv^2) and pitch angle θ. Different classes of particles have been identified. In panel A of figure 3, one shows the cross section of the velocity space ($v_{//}$, $v_{\perp}$). The different shadings correspond to different classes of orbits of particles.

The right-hand side panel (B) shows the different classes of orbits of particles at a point B located beyond the ZPF surface. Ballistic particles represented by b correspond to those particles emerging from the ion-exobase (i.e. the 1.000 km reference altitude level) which have not enough kinetic energy to reach the equatorial plane ; they fall back into the ionosphere. The escaping particles (represented by e) are those particles which have an energy larger than the potential barrier and which travel along the field line from the ion-exobase in one hemisphere to the conjugate region in the other hemisphere. In addition to these particles which emerge from the ionosphere, there are two classes of trapped particles (t1, t2) which have mirror points above the ion-exobase : t2 corresponds to orbits with two magnetic mirror points in opposite hemispheres while the t1 trapped particles correspond to particles of low energy which have reflection points in the same hemisphere, the lower one being a magnetic mirror point while the upper one being a gravitational reflection point. It can be seen that beyond the Zero Parallel Force surface (panel B) there are two new classes of trapped particles (t3, t4) corresponding to particles which are respectively magnetically and energetically trapped beyond the Zero Parallel Force surface.

Diffusive Equilibrium Density Distribution

The field-aligned density distribution given by the upper solid line in Fig.4, is obtained when all these possible orbits are populated with particles whose velocity distribution is an isothermal and anisotropic Maxwellian. This field-aligned plasma distribution corresponds to Barometric Equilibrium or Diffusive Equilibrium (DE). The different shadings in this figure show the relative abundance of the different classes of particles as a function of latitude along the field line L = 8.

Note that in a non-rotating ion-exosphere like that considered by Eviatar et al. /7/ there are no trapped particles of type t3, t4.

Indeed, for a non-rotating ion-exosphere there is no potential well near the equatorial plane along any magnetic field line : the ZPF force surface is shifted to $r = \infty$ when Ω tends to zero.

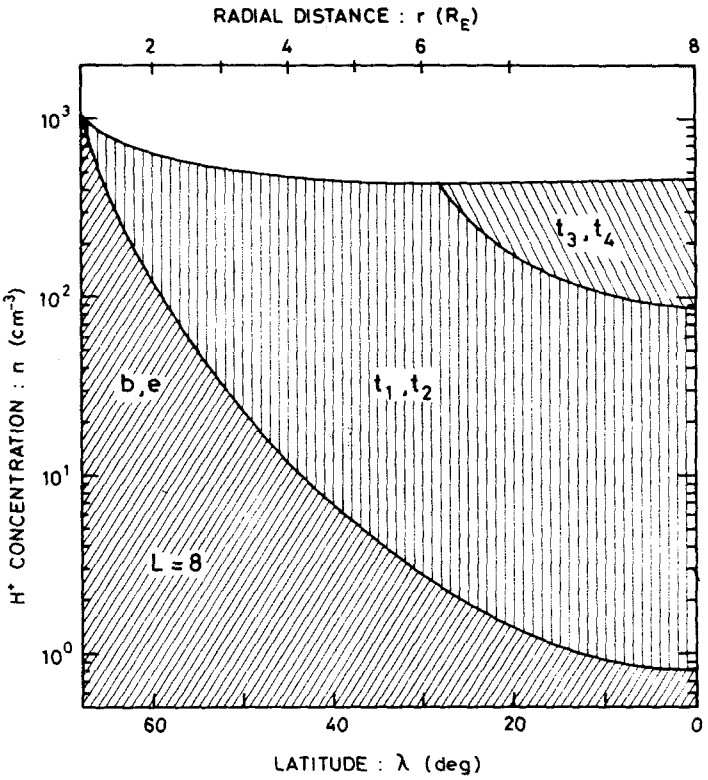

Fig.4 : Hydrogen plasma density distributions as a function of latitude (λ) along the dipole magnetic field line L = 8. The upper solid line corresponds to the Diffusive Equilibrium (DE) model for $N_o = 10^3$ cm^{-3}, T_o = 3000 K at the reference level altitude : h_o = 1000 km. The lower solid line represents the Exospheric Equilibrium (EE) kinetic model for symmetrical boundary conditions in both hemispheres. For both cases the ion-exosphere corotates with the angular velocity of the Earth. The DE density has a minimum value at the latitudes $\lambda_m = \pm 27°$ and radial distance $r_m = 6.27$ where the magnetic field line penetrates through the ZPF surface. Note the large density contributed by trapped particles to the DE distribution.

It has been estimated that a flux tube at L = 8 would need at least 66 days before the state of diffusive equilibrium can be reached via particle evaporation from the ionosphere (see lines 1 and 2 in Table 1) /10/. Whistler observations by Park /11/ had indicated that flux tubes beyond L = 4 refill very slowly and that more than 5 days are required to saturate flux tubes which have larger L values. This means that the flux tube at L = 8 will almost never reach the level of diffusive equilibrium before it experiences a new catastrophic depletion at the onset of the next magnetic substorm. This means also that magnetic flux tubes at L = 8 and more generally for L values > 4, will generally have a density which is smaller than the upper solid line in figure 4.

At the onset of a substorm the outer portion of plasmasphere is peeled off ; all flux tubes located beyond an equatorial distance of 3 or 4 Earth radii, or even less, are then completely depleted. Assuming that the density drops to almost zero, one may ask the question: how does the flux tube refill afterwards ? Or, how is the field-aligned plasma distribution evolving during the replenishment phase ?

Exospheric Equilibrium Density Distribution

From a simple kinetic point of view, it can be shown that ballistic and escaping particles (b and e class of particles) will immediately invade the empty flux tube and build up a density distribution corresponding to an Exospheric Equilibrium (EE). All this can be achieved in about one to five hours which is the characteristic time of free flight (t_F) of thermal ions along the flux tube from the 1.000 km altitude level up to the equatorial plane. The values of t_F are given in line 3 of Table 1 for different values.

TABLE 1

t_N is the flux tube refilling time for different values of L. A maximum polar wind flux of 2 x 10^8 cm^{-2} is assumed to flow at a constant rate to increase the total flux tube content from the minimum (EE) value to the diffusive equilibrium maximum value (DE) ; t_F is the free flight time of a thermal proton spiraling along the magnetic field line (L) from an altitude of 1000 km up to the equatorial plane. The proton has an energy of 0.25 eV (T_o = 3000 K) and an initial pitch angle of 45° at 1000 km altitude ; its field aligned velocity is calculated along the field line assuming conservation of the magnetic moment of the particle and conservation of the sum of kinetic energy and potential energy illustrated in Fig.2 ; t_S is the Coulomb collision time for momentum transfer of a thermal proton (0.25 eV, T ≃ 3000 K) gyrating in the equatorial plane ; the background plasma density is assumed to be equal to that of the minimum exospheric equilibrium model (n_{eq}^{EE}) /10/.

L	2	4	6	8	R_E
t_N	9.4	115	544	1587	hours
t_N	-	4.7	22.7	66.1	days
t_F	0.7	1.9	3.6	5.2	hours
t_S	0.26	2.8	10	28	hours
n_{eq}^{EE}	80	8.1	2.2	0.82	cm^{-3}

The exospheric equilibrium density is shown by the lower solid line in figure 4. Only ballistic and escaping particles are then present ; the velocity distribution is almost empty at the largest pitch angles corresponding to trapped particles t_1, t_2, t_3 and t_4. The pitch angle distribution is then strongly field-aligned and almost confined in the source cone ($0 < \theta < \theta_B$) and in the loss cone ($\pi - \theta_B < \theta < \pi$) (see figure 3).

Kinetic Refilling Process

At large pitch angles corresponding to trapped particles there should be no or almost no particles during the 1 to 5 first hours. However, since the Coulomb collision frequency is not strictly equal to zero and increases gradually as the flux tube is refilling, one can expect that higher densities are gradually building up by continuous addition and

piling up of particles on trapped orbits. Although relatively rare, Coulomb collisions are however frequent enough in the plasmasphere to scatter escaping and ballistic particles on orbits with larger pitch angles (see line 4 in Table 1). Interaction of particles with ion accoustic waves generated by possibly unstable counterstreaming ion flows may produce additional trapping of escaping or ballistic ions. Once deflected on trapped orbits at higher altitudes where the density is lowest, these particles have a lower probability for Coulomb collisions and consequently they have a tendancy to stay and accumulate there. As a result of these trapping mechanisms, the plasma density increases until eventually, after a period of several days, the flux tubes can reach the state of diffusive equilibrium discussed above and illustrated by the upper curve in figure 4.

The field-aligned distribution during the refilling process evolves between the minimum Exospheric Equilibrium and maximum Diffusive Equilibrium density distribution. An accurate description of this time evolution is a difficult numerical problem to solve. Indeed, it involves the solution of the time dependent Boltzmann equation with a non-zero collision operator.

Other scenarios for the refilling of magnetic flux tubes have been proposed by Banks et al. /4/, Singh and Schunk /16, 17/ and by Samir et al. /14/. These are based on the propagation of shocks from the ionosphere up to the equatorial plane or backwards. According to these scenarios, the whole flux tube would be refilled in a few hours of time. Observations, however, indicate that the refilling process takes place over several days /11/. These alternative scenarios with propagating hydrodynamic shocks are much faster processes than the refilling by diffusion and ionospheric evaporation which takes more than 4 days for magnetic flux tubes located beyond L = 4 (see line 3 in Table 1).

Importance of Coulomb Collisions

It is important not to underestimate the role played by Coulomb collisions as an efficient pitch angle scattering mechanism. While at the beginning of the refilling process the pitch angle distribution is mainly field-aligned and confined within the source cone and loss cone, when time goes on, the ambient plasma density increases ; more and more particles are then scattered on trapped orbits. It should also be noted that the fastest particles (i.e. the most energetic forerunners) forming the tail of the Maxwellian velocity distribution remain anisotropic and field-aligned longer than the ions with lowest energies. Indeed, the Coulomb collision cross-section for momentum transfer is energy dependent and decreases rapidly with the energy of the incident charged particles. Therefore, we expect to see the pitch angle distribution of particles with the lowest energies to become isotropic first. It is only after a much longer period of time that the suprathermal particles tend also to become more isotropic in pitch angle when the cold background density has increased to a relatively high value.

The momentum transfer Coulomb collision time (t_S) of a thermal proton (0.25 eV, T = 3000 K) gyrating in the equatorial plane is given in line 5 of Table 1 for the case when the background plasma is in exospheric equilibrium. It can be seen that at L = 4 in the equatorial plane a thermal proton of only 0.25 eV can be trapped without having a significant pitch angle deflection for almost 3 hours. At L = 8 the slowing down time t_S is 10 times longer. These values have been calculated for the minimum equatorial density corresponding to the exospheric equilibrium.

However, when during the refilling process the density approaches a diffusive equilibrium value, t_S is accordingly reduced by a large factor, e.g. : at L = 4 the diffusive equilibrium density is 60 times larger than the exospheric equilibrium density and therefore t_S is 60 times smaller (t_S = 2.8 min) than the value given in Table 1 for the case of exospheric equilibrium ; at L = 8 where the equatorial density in the exospheric

model is only 0.8 cm^{-3}, t_S is larger than one day but if diffusive equilibrium would be achieved along this field line the equatorial density would be more than 2 orders of magnitude larger and consequently t_S would be 2 orders of magnitude smaller.

These estimates show that within the plasmasphere where the density is relatively high, Coulomb collisions play an important role up the equatorial plane ; field-aligned ion beams will not be able to survive very long unless these beams are formed by suprathermal particles whose Coulomb collision cross section is significantly reduced.

However, outside the plasmasphere and in the polar wind where the density is closer to exospheric equilibrium an anisotropic velocity distribution is expected to survive for a much longer period of time even at lower thermal energies. This seems indeed to be the case according to the observation of Dynamic Explorer 1 /18, 22/.

Departures from Isotropic Pitch Angle Distributions

Table 2 gives the number of Coulomb collisions for protons and electrons injected at 1000 km altitude with an initial pitch angle (θ_o) and an initial velocity (v_o) i.e. an initial energy ($K_o = \frac{1}{2} m v_o^2$) ; q_1 is the expected number of collisions for a background plasma density distribution in diffusive equilibrium assuming that the field particles have a temperature of 3000 K and a density of 10^3 cm^{-3} at 1000 Km altitude ; q_2 is the expected number of collisions when the background density distribution is an exospheric equilibrium for the same exobase conditions. Also given in this Table is the free flight time (t_F) of the particle from the 1000 km level up to the equatorial plane.

It can be seen that thermal protons or electrons experience several collisions on their upward motion toward the equatorial plane. When the field particle density corresponds to diffusive equilibrium, the expected number of collisions (q_1) is almost 10 times larger than for the exospheric equilibrium (q_2). For suprathermal energies (K_o = 26 eV, v_o/v_T = 10, where v_T is the thermal speed of the field particles and v_o the initial velocity of the test particle) the values of q_1 and q_2 decrease rapidly below unity. This drastic reduction results from the sensitivity of the Coulomb collision cross section on the energy of the incident charged particles. Therefore it can be concluded that large departures from isotropic pitch angle distributions are expected for suprathermal protons with energies larger than 5 to 10 eV. Note also from Table 2 that protons are more effectively deflected by Coulomb collisions with field protons than with field electrons. A test electron is much more efficiently scattered by field electrons than by field protons of the same mean energy.

The electrons travel to the equatorial plane 43 times faster than the protons of the same energy (t_F is given in Table 2). But the electrons experience almost the same number of collisions as the protons. Therefore, it can be concluded that Coulomb collisions will restore isotropy of electrons velocity distribution much faster than for the thermal ions upwelling from the ionosphere.

Lemaire (1985) has also shown that the number of Coulomb collisions q_2 in an exospheric equilibrium model is almost independent of L, i.e. of the length of the magnetic field line. Indeed in the exospheric equilibrium density distribution, the background density decreases rapidly with r as r^{-4}. The lengthening of the magnetic field line with L does not contribute much to increase q_2 because along the added field line length the background density is very small. On the contrary, for a background density distribution in diffusive equilibrium the expected number of collisions (q_1) is almost 2 times larger along L = 8 than along L = 4. The free flight time (t_F) are a factor 2.8 larger at L = 8 than at L = 4.

TABLE 2

Expected number of Coulomb collisions for protons (p^+) and electrons (e^-) injected at 1000 km with a pitch angle (θ_o), an initial velocity (v_o), i.e. an initial energy (E_o) ; q_1 is the expected number of collisions for a background plasma density distribution in Diffusive Equilibrium (T_F = 3000 K and $n_F = 10^3$ cm^{-3} at 1000 km, $v_T^2 = 2\,kT_F/m$; q_2 is expected number of collisions when the background density distribution is in Exospheric Equilibrium for the same exobase conditions ; t_F is the free flight time of the test particle from the 1000 km level up to the equatorial plane along the field line L = 4 /10/.

Test particle	Field particle	v_T/v_o	K_o [eV]	θ_o	q_1	q_2	t_F [s]
p^+	p^+	1	0.26	45	55.0	6.7	6790
p^+	p^+	1	0.26	0	52.0	5.8	6450
p^+	e^-	1	0.26	45	35.3	4.9	6790
p^+	p^+	1.5	0.58	45	13.5	2.0	3190
p^+	p^+	3.0	2.33	45	0.81	0.13	1410
p^+	p^+	10	25.8	45	0.0059	0.001	409
e^-	p^+	1	0.26	45	5.15	0.36	159
e^-	p^+	1.5	0.58	45	0.24	0.032	74
e^-	p^+	3.0	2.33	45	0.0095	0.0016	33
e^-	p^+	10	25.8	45	0.000068	0.000012	9.5
e^-	e^-	1	0.26	45	55.0	6.7	159

Needs for Kinetic Descriptions

As a matter of consequence the plasma with energy below 1 eV is collision-dominated inside the dense plasmasphere ; its field aligned distribution can therefore be modelled in the framework of standard hydrodynamic approximations applicable to collision-dominated plasmas for which Chapman-Enskog's like expansions of the velocity distributions might be valid approximations.

However, a correct description of the suprathermal ions inside the plasmasphere, and a fortiori outside, requires a proper kinetic treatment based on Boltzmann's equation including the scattering effects of Coulomb collisions.

Whether additional pitch angle scattering of these warm ions by wave-particle interactions is required is not yet sure and depends on the spectral intensity of the electromagnetic waves with which these particles can resonate.

Instead of speculating about the possible importance of such wave-particle interactions, we suggest to consider in a first step the effect of Coulomb collisions and only afterwards to evaluate what remains to be explained by other alternative processes.

LIGHT ION TROUGH

Both in the ideal asymptotic state of diffusive equilibrium as well as in the exospheric equilibrium model the field-aligned density decreases with altitude, at least in the altitude range below the Zero Parallel Force, where the gravitational field is dominating the centrifugal force. Both distributions are in hydrostatic equilibrium, indeed, $\bar{v}_{//} = 0$. To maintain hydrostatic equilibrium in this region the pressure and density gradient have to be negative. It can be shown from the momentum transport equation that any reversed density gradient would lead to a Rayleigh- Taylor type instability. Indeed, one cannot maintain in hydrostatic equilibrium an atmosphere or ionosphere with densities increasing with altitudes ; such an ionosphere or atmosphere would be Rayleigh-Taylor unstable.

Upward Ionization Flow Beyond ZPF Surface

Beyond the Zero Parallel Force surface, the diffusive equilibrium density distribution increases with radial distances along the field line as can be seen in figure 4. Therefore, to maintain hydrostatic equilibrium beyond the ZPF surface, a positive density gradient is required ; a negative density distribution beyond the ZPF surface would, indeed, lead to Rayleigh-Taylor instability and drive an upward ionization flow tending to fill up the equatorial potential well. The tendancy would then be to accumulate more trapped particles in this equatorial potential well until eventually a positive density gradient is established beyond this ZPF surface. As a consequence, any field-aligned density distribution which has a negative density gradient beyond the ZPF surface gives rise to outward ionization flow near the equatorial plane. Because of the continuity equation for particle flux, upward ionization flow is expected at all altitudes down into the low altitude ionosphere where, as matter of consequences, a depletion in ionization density is expected at midlatitudes.

It has been suggested by Lemaire /10/ that field-aligned ion flow is expected not only outside the plasmasphere beyond the sharp density gradient, but also inside the plasmasphere along field lines which traverse the ZPF surface. This upward flow of H^+ ions along magnetic field lines with L-value smaller than those corresponding to the equatorial plasmapause, contributes to the formation of the Light Ion Trough (LIT) in the topside ionosphere.

Consequences of Enhanced Convection in the Post-Midnight Local Time Sector

So far we have assumed that the plasmasphere corotates with the angular velocity of the Earth. But from figure 5 it can be seen that beyond $L = 4$ and for $K_p \geq 2$, the azimuthal component of the magnetospheric convection velocity is generally enhanced by a factor of 2 or 3 in the post-midnight local time sector. This means that, in this local time sector and especially during periods of enhanced geomagnetic activity, the ZPF surface penetrates deeper into the plasmasphere than $L = 5.78$. In other words, when K_p increases, magnetospheric convection is enhanced and part of the plasmasphere becomes located beyond the ZPF surface. Considering that the density gradient along the field lines was negative before the K_p enhancement, this negative density gradient gives rise to a Rayleigh-Taylor instability ; this initiates upward ionization flow along the magnetic field line as long as it traverses the ZPF surface. This upward ionization leads to the formation of the Light Ion Trough at lower latitude in the topside ionosphere.

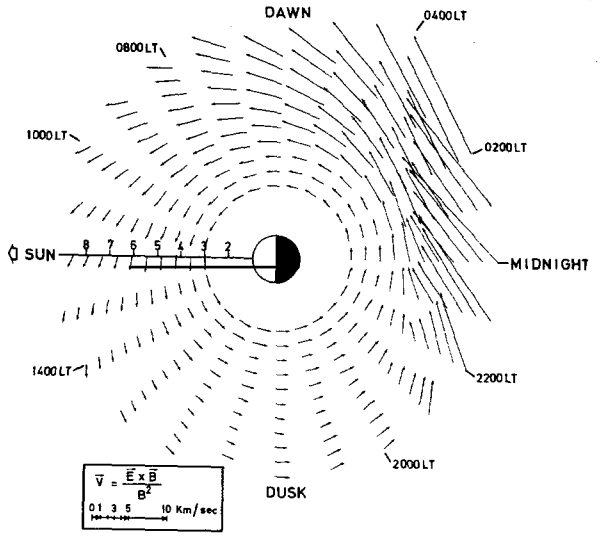

Fig.5 : Equatorial convection velocities corresponding to the electric and magnetic field models E3H and M2, in a fixed magnetospheric frame of reference. Note the large Eastward velocity component in the nightside sector corresponding to super-rotation of magnetospheric plasma. Note also the well defined noon-midnight asymmetry in the convection flow pattern /10/.

Since Hydrogen and Helium ions are the major ionic constituents at high altitudes in the magnetosphere, it is expected that this upward flow is formed of light ions only ; the heavier ones like O^+ or N^+ do not participate to the ionization upwelling in the LIT. The potential barrier given by equation (2) for the light ion is indeed much smaller than for the heavier ions which can be considered under usual circumstances to be almost in hydrostatic equilibrium and confined at lower altitudes.

Observations

It has also been found that the Light Ion Trough as well as the limit of upward ionization flow is shifted toward lower latitudes when K_p is enhanced /20, 19, 1/. Evidence of upward ionization flow at L values smaller than the equatorial plasmapause is illustrated in figure 6 taken from Titheridge /21/.

The dashed line in figure 6 shows the local time L-values and geomagnetic latitudes of the equatorial plasmapause determined from whistler measurements for $K_p \leq 3^+$. The latitude of the low altitude projection of the plasmapause, as identified by a peak in the plasma temperature of the topside ionosphere, is indicated by the P's at the upper edge of the light shaded zone. The low latitude edge of this shaded area is indicated by A's ; it represents the latitudes below which no upward ionization flow can be inferred from the O^+/H^+ transition heights and from the electron density variation with latitude (see Titheridge /23/). In this shaded region the O^+/H^+ transition height (h_T) is above

the height for chemical equilibrium (h_c) ; consequently there is an upflow of H^+ ions ($F_{//}$) which increases with latitude. Between the latitudes indicated by A's and B's, h_T and $F_{//}$ increase with latitude rather slowly ; but between the B's and P's in figure 6, the slope of this variation becomes suddenly steeper by a factor larger than 2.

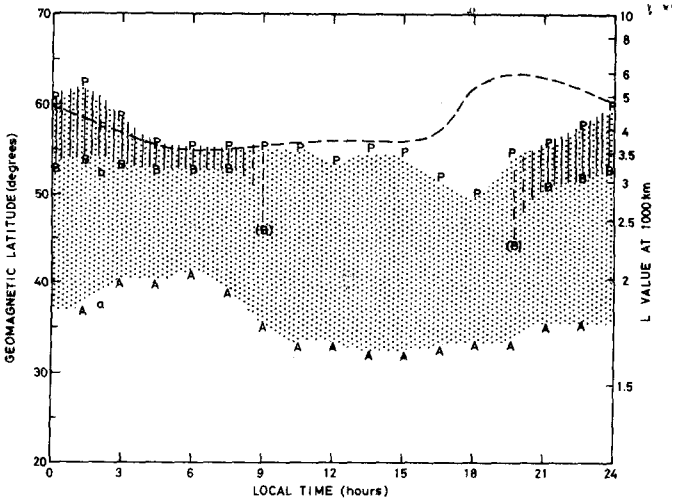

Fig.6 : The dashed line illustrates the local time dependence of the equatorial plasmapause positions as determined from whistler observations. The P's correspond to the low altitude projection of the plasmapause as identified by the peak in the plasma temperature distribution as a function of geomagnetic latitudes. The shaded zone between the A's and P's correspond to a region of upward ionization flow with field aligned flux increasing slowly between the latitudes λ_A and λ_B ; λ_B is the minimum latitude where the observed O^+/H^+ transition heights indicate that the upward ionization flux has reached the maximum Polar Wind flux. In the hached zones between the latitudes λ_B and λ_P, a limiting upward Polar Wind flux of H^+ ions is inferred from the high altitude of h_T, the observed O^+/H^+ transition heights /21/.

In this outer shell of the plasmasphere the upward light ion flux increases more rapidly with latitude than between the A's and B's. But this change in the slope of h_T and F is only observed in the 2000 LT to 0600 LT sector. As a result of the squeezing of the magnetic flux tube in these local time sectors one should, however, expect a downward flow of ionization instead of the upward one observed.

But this usual reasoning does not take into account that at nightside local times plasma elements are accelerated along their drift path and have, after 2000 LT, angular velocities Ω larger than the angular velocity of the Earth (Ω_E) (see Fig.5). Therefore the centrifugal force becomes increasing dominant along the plasma streamlines. This leads in the nightside sector to the formation of the above mentioned potential well near the equatorial plane (see Fig.2).

To fill up this potential well developing in the nightside beyond the ZRF surface, a larger uprush of fresh plasma from the ionosphere is required for all magnetic field lines beyond the latitudes B and P shown in figure 6. This is a plausible explanation for the observations of the unexpected upward ionization flow in the nightside local time sector, where downward flow was generally expected /21/.

EQUATORIAL DENSITIES

So far we have examined the centrifugal effects of non-uniform angular velocities and a mechanism for the formation of a nightside LIT along geomagnetic field lines which traverse the ZPF surface. There are other possible dynamical effects resulting from diurnal contractions and expansions of magnetic flux tubes due to perpendicular plasma transport in the plasmasphere.

Equatorial Drift Paths

The equatorial drift path of three plasma elements are shown in figure 7. Their drift velocity, shown in figure 5, has been calculated from McIlwain's electric and magnetic models E3H and M2.

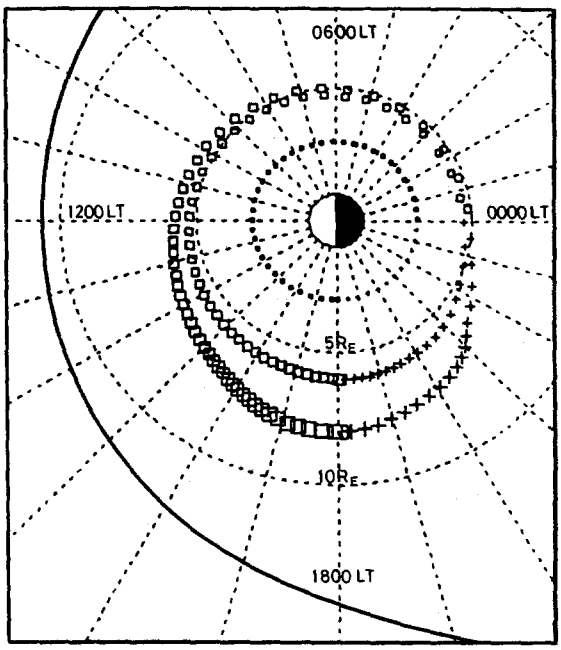

Fig.7 :Drift path of three plasma elements in the electric and magnetic field distributions E3H and M2, respectively. The series of symbols indicate their successive positions each half hour interval of time. The size of these symbols changes along the drift path to indicate the variation of the equatorial cross section (S_{eq}) of the plasma element : $S_{eq}(L,\phi)$ is inversely proportional to the equatorial magnetic field intensity, $B_{eq}(L,\phi)$. The type of symbols representing the plasma element changes when it traverses the midnight meridional plane (ϕ = 0000 LT, 2400 LT...). These closed drift trajectories are parallel to equipotential lines of the stationary E3H electric field. The radial distance for these three drift paths is maximum in the dusk local time sector, respectively at 8 R_E, 6 R_E and 3 R_E /10/.

Let us now examine diurnal variations of the equatorial density inside these plasma elements convecting along drift paths which are not necessarily parallel to a geomagnetic L-shell. Ignoring cross-B diffusion processes, as well as plasma interchange motion, the theorem of conservation of magnetic flux tells us that the equatorial cross section (S_{eq}) of the field aligned plasma elements varies as B_{eq}^{-1} along its drift trajectory. The sizes of the symbols (□,+) used in figure 7 to indicate the positions of drifting plasma elements every half hour of Universal Time (UT) is proportional to the instantaneous cross-section (S_{eq}) of the plasma elements. As a consequence of the dawn-dusk asymmetry of its drift path, the cross section of the outermost plasma element

shrinks significantly when it penetrates in a region of higher magnetic field intensity. During this almost adiabatic contraction, the plasma density and temperature increase. Conversely, when these plasma elements move outwardly toward regions with lower magnetic field intensity, their equatorial cross-section and their density are respectively increasing and decreasing as

$$S_{eq}(L) \propto B_{eq}^{-1} \tag{3}$$

$$n_{eq}(L) \propto V^{-1} \tag{4}$$

where V(L) is the volume of the plasma element which is almost equal to the volume of the magnetic flux tube containing this field aligned element.

The distances between successive half-hour positions of the drifting plasma elements shown in figure 7 are inversely proportional to the convection velocity ($\underline{V}_E = \underline{E} \times \underline{B}/B^2$). It can be seen that along the post-dusk portion of the outermost trajectory the convection velocity is significantly enhanced. Along the dayside and dusk portions of the two outermost trajectories, the spacing between successive positions is smaller, indicating the slowing down of plasma elements. The enhanced convection velocity in the post-midnight sector, is shown in figure 5.

The diminishing size of the symbols along the post-dusk portion of the trajectory illustrates the contraction or squeezing of the plasma element while it drifts toward local midnight and closer to the Earth.

The innermost plasma element drifts around the Earth's in 24 hours along an almost circular trajectory. Indeed when K_p is less than 2, corotation prevails up to L = 4. The second plasma element orbiting at intermediate radial distances circulates around the Earth in 32 hours, while the outermost one takes 34 hours to complete a revolution. It is evident from these simulations that the trajectories of plasma elements located in the inner plasmasphere are nearly symmetric, while those circulating in the outermost part of the plasmasphere become increasingly asymmetric. Lemaire /10/ has examined the consequences of this increasing geometrical asymmetry for the equatorial density (n_{eq}), for the total flux tube content (N_T), as well as for the average ion temperatures ($T_\parallel$ and $T_\perp$) and for temperature anisotropy ($T_\perp/T_\parallel$). We will only present here the major conclusions concerning the diurnal variation of n_{eq}. They are illustrated in figure 8.

Field Aligned Flux

For all three plasma elements whose trajectories are shown in figure 7 the numerical integration has been started with very low initial equatorial densities at time t = 0, when all three elements were located in the dusk local time sector (ϕ = 1800 LT) respectively at L = 8, 6 and 3 for the elements a, b and c. Upward ionization flux F is assumed to refill gradually the almost empty plasma elements ; the maximum value of field aligned flux being the limiting polar wind H^+ flux :

$$F_{max} = N_o(kT_o/2\pi m)^{1/2} \tag{5}$$

where N_o and T_o are the H^+ ion density and temperature at the reference altitude of 1000 km (ion-exobase). For $N_o = 10^3$ cm^{-3} and T_o = 3000 K one obtains $F_{max} = 2 \times 10^8$ cm^{-2}s^{-1}. The actual upward flux F is given in the numerical calculations by

$$F = \alpha F_{max}(n_{eq}^{DE} - n_{eq})/n_{eq}^{DE} \tag{6}$$

where $n_{eq}^{DE}(L,\phi)$ is the saturation equatorial density for diffusive equilibrium (DE) in the flux tube L ; $n_{eq}(L,\phi)$ is the actual equatorial density in that same flux tube at

time t when the plasma element is at local time $\phi(t)$, α is constant factor which is set equal to zero in simulations when no ionization is assumed to flow between the ionosphere and the magnetosphere ; α is assumed to be equal to 1 for the simulations illustrated in figure 8, in order to model upward ionization with limiting Polar wind fluxes.

Diurnal Variation of the Equatorial Density and Flux Tube Refilling

Figures 8a, b and c show variations of $n_{eq}[L(t),\phi(t)]$ for the three plasma elements convected along the three drift paths illustrated in figure 7. The abscissa gives the local time $\phi(t)$ of the element at the universal time t. At the initial time t = 0 the plasma elements were all located at ϕ_o = 1800 LT but at different equatorial distances (L_o = 8, 6 and 3) ; their initial equatorial densities were respectively equal to 0.8 cm^{-3} for the outermost one (a), 2.5 cm^{-3} for the intermediate one (b) and 41 cm^{-3} for the innermost one (c). As in figure 7 the variable size of the symbols indicates the variation of the equatorial cross-section of the plasma element assuming that their magnetic flux is conserved, the larger the size of these symbols the smaller becomes L(t). The equatorial densities corresponding to Diffusive Equilibrium (n_{eq}^{DE}) are given by the solid curve near 450 cm^{-3}. This would be the equatorial density if the flux tube would be saturated and if all classes of particles would be in thermal equilibrium with those emerging from the ionosphere.

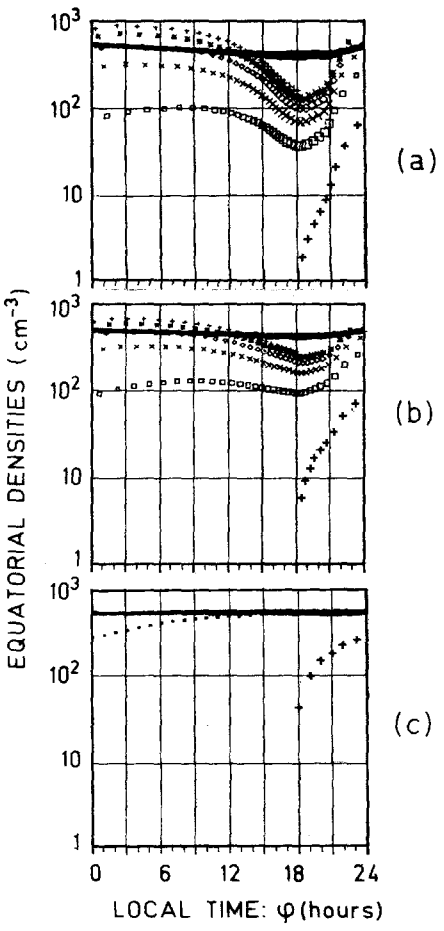

Fig. 8

Fig.8 :Equatorial density (n_{eq}) in three plasma elements drifting in the E3H + M2 electric and magnetic field distribution along the trajectories illustrated in figure 7. The series of symbols indicate the successive values of n_{eq} as a function of local time (ϕ) for every half hour interval of Universal Time (t). The size of these symbols changes along the closed drift path to indicate the variation of the equatorial cross section (S_{eq}) of the plasma element. The type of symbols representing the equatorial density changes each time when the plasma element traverses the meridional plane (ϕ = 0000 LT, 2400 LT, 4800 LT, ...). The solid line near 450 cm^{-3} in each panel gives the equatorial density in the magnetic flux tube if Diffusive Equilibrium (DE) would be achieved. In these simulations ions flow upwards as long as n_{eq} is smaller than the DE value ; (a) the upper panel illustrates the slow refilling rate which is superimposed on a large amplitude diurnal variation for a plasma element whose initial equatorial density is 0.8 cm^{-3} at L = 8 and ϕ = 1800 LT ; (b) ibidem for 2.5 cm^{-3} at t = 0 and L = 6 in the duskside ; (c) ibidem for n_{eq} = 41 cm^{-3} at t = 0 and L = 3, and ϕ = 1800 LT (lower panel). /10/.

When n_{eq} exceeds n_{eq}^{DE} the field-aligned flux given by equation (6) becomes negative ; plasma stored in the plasmasphere is then dumped into the ionosphere. This is precisely what happens between 0000 and 1200 LT to the outermost plasma element (a) after several days of refilling, more precisely after its fourth revolution around the Earth. The same happens even earlier to the intermediate element b.

Figures 8a, b and c illustrate that the outermost flux tube (a) drifting at 8 R_E takes more than 7 days (i.e. more than 5 revolutions around the Earth) to refill, while the innermost one drifting at L = 3 takes only 24 hours (i.e. 1 revolution) to complete Diffusive Equilibrium. Note that these simulations have been carried out with $\alpha = 1$ (i.e. for the maximum field aligned refilling flow which is equal to the limiting polar wind flux. A smaller value of α would of course increase the refilling times (t_N) accordingly. Refilling times calculated with $\alpha = 1/2$ would be closer to those deduced by Park /11, 12/ from whistler observations.

Note that in the afternoon and dusk sectors the equatorial density is generally smaller than in the pre-noon sector. The amplitude of the diurnal variation superimposed on the slow refilling of the magnetic flux tube is much larger along the outermost drift path (Fig.8a) than along the innermost one (Fig.8c) as a consequence of the larger dawn-dusk asymmetry of the outermost convection streamlines. This indicates that the largest diurnal variation of equatorial densities is expected in the outer region of the plasmasphere.

During periods of enhanced geomagnetic activity the amplitude of this diurnal variation increases even more rapidly with L as a consequence of the enhanced dawn-dusk asymmetry of the convection streamlines when K_p is large.

As a result of the flux tube contraction in the post-dusk sector n_{eq} eventually exceeds n_{eq}^{DE} : values larger than 930 cm^{-3} are obtained at L = 4.8 when the outermost plasma element drifts in the post-midnight sector. On the contrary at dusk, where the trajectory has its maximum extent, the minimum equatorial density in the final stationary regime, is equal to 134 cm^{-3} at L = 8. Both the value of the post-midnight maximum (930 cm^{-3} at L = 4.8) and the value of the dusk minimum (134 cm^{-3} at L = 8) are larger than the observed values by a factor of 3 or 4 /5, 6,13/.

PLASMASPHERIC WIND

A simple way to reduce the overall equatorial density in the outer plasmasphere is to consider that the plasmasphere is continuously expanding like the solar corona, and that this continuous radial expansion forms a subsonic 'plasmaspheric wind' somewhat similar to the coronal expansion. Indeed, as a consequence of such a radial plasmaspheric wind, the equatorial density would decrease faster with L than the value corresponding to diffusive equilibrium. From the equation of conservation of the total plasma content in flux tubes expanding outwardly in a dipole magnetic field, it results that the equatorial background (BG) density distribution should vary almost as L^{-4} : i.e. as the inverse of the flux tube volume V :

$$n_{eq}^{BG}(L) = D/L^4 \qquad (7)$$

Such a characteristic L^{-4} equatorial density profile is often observed in the outer plasmasphere. The constant D in equation (7) can be determined empirically from the observations which show that the background plasma density at L = 4 is often equal to 500 ions/cm^3. It results then from equation (7) that $D = 1.28 \times 10^5$ ions/cm^3.

Note, however, that the equatorial density distribution OF a slowly expanding plasmasphere would be in between that corresponding to Diffusive Equilibrium for which the expansion velocity is equal to zero, and the L^{-4} distribution corresponding to a fast

adiabatic radial wind. The upper limit of the velocity of this plasmaspheric expansion would be equal to the maximum interchange velocity which is inversely proportional to the value of the integrated Pedersen conductivity. Therefore, realistic models of such a plasmaspheric wind requires also a detailed description of ionosphere-magnetosphere coupling processes (i.e. dissipation of potential energy by Joule heating, as well as field-aligned refilling processes)

Evidence for a continuous plasmaspheric wind can also be found in figure 6 obtained by Titheridge /21/. Indeed, in the shaded region between the latitudes λ_A and λ_P, the actual altitude h_T of the O^+/H^+ transition is higher than the corresponding altitude for chemical equilibrium at all local times. Since this implies upward ionization flow at all local times, it can be concluded that along all field lines of the outer plasmasphere light ions are flowing upwards at all local times (see figure 6). Such an incessant field aligned flow cannot be sustained without an equal outward radial flow across magnetic field lines, i.e. either without a continuous plasmaspheric wind, or, without frequent sporadic losses of plasma by substorm associated peelings off of the plasmasphere, deep inside, down to L-shells of $L_A = 2 - 1.7$ (i.e. down to invariant latitudes $\lambda_A = 40 - 35°$ as shown in figure 6).

Park /11/ has also shown from whistler observations, that under quiet geomagnetic conditions, the observed rate of increase in daytime flux tube content gives an upward flux of 3×10^8 electrons/cm^2/s at the 1000 km altitude level ; this is larger than the downward flux necessary to maintain the nocturnal ionosphere i.e. 1.5×10^8 electrons/cm^2/s. Since there are more ions flowing upward into the plasmasphere during the day than returning to the ionosphere during the night one can again be lead to conclude that there should be a continuous plasmaspheric wind with subsonic expansion velocities, or else, frequent and deep plasmasphere erosion events.

ACKNOWLEDGEMENTS

I wish to thank C.R. CHAPPELL for the useful comments and editing of the manuscript. I wish also to thank the Fonds National de la Recherche Scientifique for financial support.

REFERENCES

1. M. AHMED, R.C. SAGALYN, P.J.L. WILDMAN, and W.J.BURKE, Topside ionospheric trough morphology : occurrence frequency and diurnal, seasonal and altitude variations, J. Geophys. Res., 84, 489-498, 1979.
2. H. ALFVEN, On frozen-in field lines and field-line reconnection, J. Geophys. Res., 81, 4019-4021, 1976.
3. J.J. ANGERAMI, and D.L. CARPENTER, Whistler studies of the plasmapause in the magnetosphere. 2. Electron density and total tube electron content near the knee in magnetospheric ionization, J. Geophys; Res., 71, 711-725, 1966.
4. P.M. BANKS, A.F.NAGY and W.I.AXFORD, Dynamical behavior of thermal protons in the mid-latitude ionosphere and magnetosphere, Planet. Space Sci., 19, 1053-1067, 1971.
5. C.R. CHAPPELL, K.K. HARRIS and G.W. SHARP, A study of the influence of magnetic activity on the location of the plasmapause as measured by OGO 5, J. Geophys. Res., 75, 50-56, 1970a.
6. C.R. CHAPPELL, K.K. HARRIS and G.W.SHARP, The morphology of the bulge region of the plasmasphere, J. Geophys. Res., 75, 3848-3861, 1970b.
7. A. EVIATAR, A.M. LENCHEK, and S.F. SINGER, Distribution of density in an ion-exosphere of a nonrotating planet, Phys. Fluids, 7, 1775- 1779, 1964.

8. J. LEMAIRE, The "Roche-limit" of ionospheric plasma and the formation of the plasmapause, Planet. Space Sci., 22, 757-766, 1974.
9. J. LEMAIRE, Rotating ion-exospheres, Planet. Space Sci., 24, 975-985, 1976.
10. J. LEMAIRE, Frontiers of the plasmasphere, Thèse d'agrégation de l'Enseignement Supérieur, UCL, Ed. Cabay, Louvain-la-Neuve, Aeronomica Acta A, 298, 1985.
11. C.G. PARK, Whistler observations of the interchange of ionization between the ionosphere and the protonosphere, J. Geophys. Res., 75, 4249-4260, 1970.
12. C.G. PARK, Some features of plasma distribution in the plasmasphere deduced from Antarctic whistlers, J. Geophys. Res., 79, 169-173, 1974.
13. C.G. PARK, D.L. CARPENTER and D.B. WIGGIN, Electron density in the plasmasphere : whistler data on solar cycle, annual, and diurnal variations, J. Geophys. Res., 83, 3137-3144, 1978.
14. U. SAMIR, K.H. WRIGHT, Jr. and N.H. STONE, The expansion of a plasma into a vacuum : basic phenomena and processes and applications to space plasma physics, Rev. Geophys. Space Phys., 21, 1631-1646, 1983.
15. M. SCHULZ and H.C.KOONS, Thermalization of colliding ion streams beyond the plasmapause, J. Geophys. Res., 77, 248-254, 1972.
16. N. SINGH and R.W. SCHUNK, Numerical calculations relevant to the initial expansion of the polar wind, J. Geophys. Res., 87, 9154-9170, 1982.
17. N. SINGH and R.W. SCHUNK, Numerical simulations of counterstreaming plasmas and their relevance to interhemispheric flows, J. Geophys. Res., 88, 7867-7877, 1983.
18. J.J. SOJKA, R.W. SCHUNK, J.F.E. JOHNSON, J.H. WAITE and C.R. CHAPPELL, Characteristics of thermal and suprathermal ions associated with the dayside plasma trough as measured by the Dynamics Explorer retarding ion mass spectrometer, J. Geophys. Res., 88, 7895-7911, 1983.
19. H.A. TAYLOR, Jr., H.C. BRINTON, M.W. PHARO, III and N.K. RAHMAN, Thermal ions in the exosphere ; evidence of solar and geomagnetic control, J. Geophys. Res., 73, 5521-5533, 1968.
20. H.A. TAYLOR, Jr. and W.J. WALSH, The light-ion trough, the main trough and the plasmapause, J. Geophys. Res., 77, 6716-6723, 1972.
21. J.E. TITHERIDGE, Plasmapause effects in the topside ionosphere, J. Geophys. Res., 81, 3227-3233, 1976.
22. J.L. HORWITZ, R.H. COMFORT and C.R. CHAPPELL, Thermal ion composition measurements of the formation of the new outer plasmasphere and double plasmapause during storm recovery phase, Geophys. Res. Letters, 11, 701-704, 1984.